Flow reactor oxidation of ammonia-hydrogen fuel mixtures

Maria U. Alzueta,[†] Victor Mercader,[†] Alberto Cuoci,[‡] Sander Gersen,[¶] Hamid Hashemi,[§] and Peter Glarborg*[,§]

†*Aragon Institute of Engineering Research (I3A). Department of Chemical and Environmental Engineering, University of Zaragoza, 50018 Zaragoza, Spain*

‡*Department of Chemistry, Materials, and Chemical Engineering "G. Natta", Politecnico di Milano, Milano 20133, Italy*

¶*DNV Oil & Gas, P.O. Box 2029, 9704 CA Groningen, The Netherlands*

§*DTU Chemical Engineering, Technical University of Denmark, 2800 Lyngby, Denmark*

E-mail: pgl@kt.dtu.dk

Abstract

Hydrogen-assisted oxidation of ammonia under flow reactor conditions was investigated through experiments and chemical kinetic modeling. Novel experiments, conducted in a tubular laminar flow reactor as a function of NH_3/H_2 ratio, stoichiometry, and temperature (725-1475 K), were analyzed along with literature results from tubular and jet-stirred flow reactors. Ignition and oxidation of NH_3 is strongly promoted by presence of H_2 under all conditions investigated. In general, the behavior is captured well by the kinetic model. With an increasing fraction of H_2 in the fuel mixture, the generation of chain carriers gradually shifts from being controlled by the amine reaction subset to being dominated by the oxidation chemistry of H_2, which is known more accurately. However, under reducing conditions the H_2 consumption rate is strongly underpredicted. This short-coming suggests that the

thermochemistry of amine radicals and/or the formation of higher amines need further assessment. The present analysis shows that for lean oxidation of NH_3/H_2 mixtures in tubular flow reactors, data obtained at higher temperatures, particularly for NO formation, may be strongly affected by reaction during preheating or by mixing (dependent on reactor design) in the inlet section prior to the isothermal zone. Modeling predictions for the high pressure, medium temperature ignition conditions in a large diesel engine indicate that NH_3/H_2 fuel mixtures may still require a co-fuel to secure stable ignition.

1. Introduction

Climate change, security of energy supply, and fossil fuels depletion provide an incentive for a transition to a low-carbon economy. Ammonia is a carbon-free fuel and can be a suitable alternative for stationary power, transportation, and energy storage applications. Challenges of using ammonia in engines and gas turbines are investigated extensively.[1–3] There has been a number of studies on the use of NH_3 as an engine fuel, but its poor combustion characteristics for conventional engine combustion techniques have been difficult to overcome. Hence, additional fuels such as hydrogen, natural gas, or diesel have been suggested as combustion promotors.[4,5] In particular hydrogen is interesting as a co-fuel,[6–8] because it is carbon-free and may possibly be produced from cracking ammonia in a pre-combustion process.

Predictions of ignition, burnout and pollutant emissions are dependent on reliable chemical mechanisms. There are numerous recent kinetic models for ammonia oxidation available, including those of Mathieu and Petersen,[9] Li et al.,[10] Otomo et al.,[11] Glarborg et al.,[12] Mei et al.,[13,14] Stagni et al.,[15] and Jiang et al.[16] Still, schemes that offer accurate predictions over a wide range of conditions are scarce.[3] The short-comings of the NH_3 models may be less pronounced when NH_3 is co-combusted with a second fuel, because the radical pool will be partly governed by the oxidation of the additive fuel, which in the case of H_2 is known

quite accurately.

A significant number of experimental studies of oxidation of NH_3/H_2 have been reported, many of them very recently. Aganesyan and Nalbandyan[17] reported the effect of NH_3 addition on the first ignition limit for H_2/O_2 mixtures in a batch reactor. The structure of premixed $NH_3/H_2/O_2$ flames was investigated in a series of papers by Vandooren,[18–20] while flame speed measurements are available from several research groups.[14,21–35] Also the stability and extinction of flames fueled by NH_3/H_2 mixtures have been evaluated.[36–38] Ignition delay times have been reported from rapid compression machine (RCM) studies at medium temperatures and elevated pressure[39–42] and from shock tube work at higher temperatures.[43–45] The oxidation behavior of NH_3/H_2 mixtures have been studied in flow reactors[45–50] and recently also in jet-stirred reactors.[51–56]

The purpose of the present work is to investigate the oxidation of NH_3/H_2 in flow reactors. Contrary to measurements of ignition delay times and laminar flame speeds that provide information relevant for the early stages of combustion, the flow reactor characterizes the chemistry occurring at longer time-scales, the post-flame oxidation rate and formation of pollutants. In the present work, experimental data coming from different reactor types are analyzed and interpreted on the basis of a unique kinetic mechanism. Novel experiments are conducted in a non-premixed flow reactor (preheating prior to mixing), and literature results obtained in premixed tubular reactors (mixing prior to preheating) and jet-stirred reactors are included in the analysis. The experimental data are interpreted in terms of the recent reaction mechanism by Jian et al.[57] Possible experimental artifacts, mainly related to the high reactivity and diffusivity of H_2, that may influence the interpretation of the results are analyzed and discussed. The paper is organized as follows. Sections 2 and 3 contain descriptions of the chemical kinetic model and experimental procedures, respectively. Section 4 contains subsections on analysis of the present experimental work in a non-premixed reactor (4.1), as well as literature results from premixed tubular reactors (4.2), jet-stirred reactors (4.3), and premixed laminar flame (4.4). In section 4.5, the kinetic modeling is

analyzed, while section 4.6 contains a discussion of the practical implications for NH_3/H_2 co-combustion.

2. Detailed Chemical Kinetic Model

The chemical kinetic model, including rate coefficients and thermodynamic data, is adapted from the recent study of NH_3 oxidation by Jian et al.[57] The core of the mechanism is drawn from the review of nitrogen chemistry by Glarborg et al.,[12] but with modifications based on more recent work.[58,59] The H_2-O_2 subset[60,61] was updated according to the work of Klippenstein and coworkers on chemically termolecular reactions H + O_2 + R[62] and on HO_2 + HO_2.[63] The amine subset was revised based on work on NH_2 + H (+M),[64,65] NH_3 + HO_2,[15] NH_2 + O,[66] NH_2 + HO_2,[64,67] as well as steps in the diazene,[68] H_2NO,[69] and HNO[57,66] subsets.

In combustion of ammonia with or without co-fuels, it is important to consider the collision efficiency of ammonia compared to other molecules. Recent work by Jasper and coworkers has shown that ammonia has a significantly higher third body efficiency than Ar and N_2 for the reactions NH_3 + M,[64] N_2H_4 + M,[64] and HNO + M.[57] This also apply for the pressure dependent reactions in the H_2/O_2 subset, in particular H + O_2 + M, where NH_3 has a collision efficiency 18-20 times higher than that of Ar.[70]

3. Experiments

Experiments were conducted in a non-premixed laminar flow reactor setup operated at atmospheric pressure. A detailed description of the experimental procedure can be found elsewhere.[59,71–73] Reactants (NH_3, H_2, and O_2, highly diluted in nitrogen), were fed from gas cylinders through mass flow controllers and led to a quartz tubular flow reactor in four separate streams, following the procedure of Alzueta et al.,[74] and then mixed at the entrance to the reaction zone. The reactor (0.87 cm internal diameter) was heated electrically by means

of an oven with three heating zones. At the outlet of the reactor, reaction was quenched by adding air through an external refrigeration jacket. Experiments were conducted using a constant total flow rate of 1.0 L/min (298 K, 1 atm). This way, the gas residence time in the isothermal zone of the reactor varied with temperature. At the outlet of the reactor, gases were analyzed using a Fourier Transform Infra-red (FTIR) spectrometer (Protea, ProtIR 204M) for NH_3 and NO, a micro-chromatograph (GC) with TCD detectors (Agilent Technologies 490) for NH_3, H_2, and O_2, and a continuous analyzer (ABB advance optima) for O_2. The uncertainty of the measurements is estimated to be within 5%, and not less than 5 ppm, for the continuous analyzers, and 10 ppm for the GC.[72,73]

4. Results and Discussion

Flow reactor studies of oxidation of NH_3/H_2 mixtures have been reported by several groups[45–50] and novel data are presented in the present work. In kinetic analysis of these experiments, there are potential experimental artifacts that are important to address. The issues include uncertainties in temperature and breakdown of the plug-flow approximation due to the high reactivity and fast diffusivity of hydrogen. Surface reactions, reported to shorten the induction time of lean NH_3 oxidation in laminar flow quartz reactors,[12,57,75] are presumably insignificant for NH_3/H_2 mixtures due to the high gas-phase reactivity of hydrogen.

In the following, flow reactor results on the oxidation of NH_3/H_2 mixtures in tubular flow reactors are interpreted in terms of the detailed kinetic model, taking into account the complexities of the experiment. We distinguish between *premixed flow reactor experiments*, where the reactants are mixed prior to heating, and *non-premixed flow reactor experiments*, where the reactants are heated separately and mixed at the entrance to the isothermal zone of the reactor. In the present work, the experiments on NH_3/H_2 oxidation were conducted in a non-premixed reactor, while results from literature were all obtained in tubular reactors with mixing prior to heating. Modeling predictions are also compared to selected data

from jet-stirred reactors, rapid compression machines (RCM), and laminar premixed flames. Most of the modeling was conducted with the Chemkin-PRO software, which is part of the ANSYS Fluent package.[76] However, selected 0D and 1D calculations were performed in the OpenSMOKE++ Suite,[77,78] while laminarSMOKE++[79,80] was used for the 2D simulations.

4.1 Non-premixed flow reactor results

In the present work, we have conducted flow reactor experiments on NH_3/H_2 oxidation using a non-premixed tubular reactor.[71–73,81] In this design, reactants are preheated separately, eliminating reaction prior to the isothermal zone. These type of experiments are generally modeled assuming isothermal plug-flow. However, since the gases enter the reactor unmixed, the mixing region becomes important at high reaction rates. Kristensen et al.[81] estimated the mixing time in a similar reactor to be of the order of 5 ms. The value depends on the reactor design and size, and does not account for back-mixing upstream of the injecion location. Furthermore, both atomic and molecular hydrogen have large diffusion coefficients, which may cause breakdown of the plug-flow assumption.

To evaluate the impact of modeling assumptions, we conducted flow reactor simulations, investigating the accuracy of an isothermal plug-flow assumption. The following modeling approaches were tested:

- Conventional isothermal plug flow reactor (PFR).
- 1D tubular reactor with laminar axial diffusion, with prescribed uniform temperature on the wall and accounting for back-diffusion across the section (Danckwert's boundary conditions).
- 1D-Taylor-Aris: 1D tubular reactor with enhanced axial diffusion according to the Taylor-Aris correlation.[82]
- 2D axisymmetric reactor with back-diffusion.

Our analysis indicates that under the very dilute conditions of the present experiments, the assumption of isothermal plug flow is generally met, except at high temperature where the plug-flow assumption breaks down. For conditions with excess O_2, this has no implications for the prediction of the overall oxidation, as both NH_3 and H_2 are depleted before exiting the isothermal zone, but it has a major impact on the calculated NO.

Figure 1 shows the effect of modeling assumptions on predictions for oxidation of a lean NH_3/H_2 mixture as a function of time at 1300 K. Several important observations can be made. The predicted NH_3 oxidation depends slightly on the modeling assumptions, but in all cases it occurs within 5 ms. Thereby, the reaction time is comparable to the mixing time and the experimental results are likely to be mixing influenced. Furthermore, break-down of the plug-flow assumption has implications for NO. While the PFR modeling and the 1D prediction show similar levels of NO, the introduction of the additional Taylor-Aris diffusion term or using a full 2D simulation serve to decrease NO by about 25%. Compared to the 1D simulation, the Taylor-Aris correction augments the importance of back-diffusion, which is the main reason for the decrease in the NO formation. For the 2D simulation, the difference in NO arises mainly from diffusional effects.

On the basis of these results, it seems that both mixing and axial diffusion play a role for the NO formation. At 1300 K, the measured mole fraction of NO is only about 70 ppm, while the full 2D simulation yields a value of about 275 ppm. Even though kinetic uncertainties may contribute, we attribute most of this discrepancy to the effect of reactant mixing, which is not accounted for in the modeling. As a result, we abstain from comparing modeling predictions with experiment for NO and N_2O, but the measured values are available as Supplementary Information.

To ensure that the measured overall oxidation behavior were unaffected by experimental artifacts, selected experiments were repeated in different reactors. Results for oxidation of an NH_3/H_2 mixture under reducing conditions obtained in reactors of different material (quartz or alumina) agreed closely. The current experiments were conducted at comparatively low

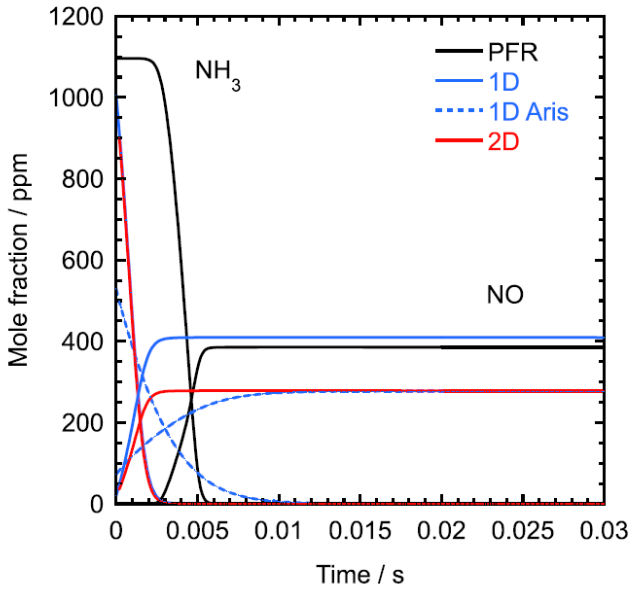

Figure 1: Impact of modeling assumptions on predictions for oxidation of an NH_3/H_2 mixture in an atmospheric pressure, isothermal tubular flow reactor (no preheating zone). Conditions: NH_3 = 1096 ppm, H_2 = 1852 ppm, O_2 = 3617 ppm; balance N_2, T = 1300 K, reactor residence time = 0.15 s. The measured exit levels of NH_3 and NO were 0 ppm and 72 ppm, respectively. Notation: PFR (plug flow), 1D (1D reactor with laminar axial diffusion), 1D AT (1D reactor with enhanced axial diffusion according to the Taylor-Aris correlation), and 2D (full 2-dimensional, axisymmetric reactor).

O_2 concentrations, reducing the initial reaction rate and largely eliminating reaction in the mixing zone, except at high temperature.

Figure 2 compares the measured and predicted mole fractions of NH_3, H_2, and O_2 in oxidation of a mixture with about 1000 ppm NH_3 and 1000 ppm H_2 under reducing conditions (excess air ratio $\lambda = 0.6$). Results are shown for three experimental runs conducted under similar conditions. The repetivity is good. Of particular interest is the H_2 concentration, which proved challenging to capture by the model, as discussed below. The measured H_2 profiles are largely identical among the different runs. Furthermore, when adding/removing the H_2, the concentration rapidly stabilizes and no hysteresis is observed.

Reaction is initiated at ~1000 K. Above this temperature, the concentrations of NH_3 and O_2 decrease monotonically with increasing temperature, while H_2 has a minimum around 1100 K. Since the conditions for the three sets are very similar, only one set of modeling

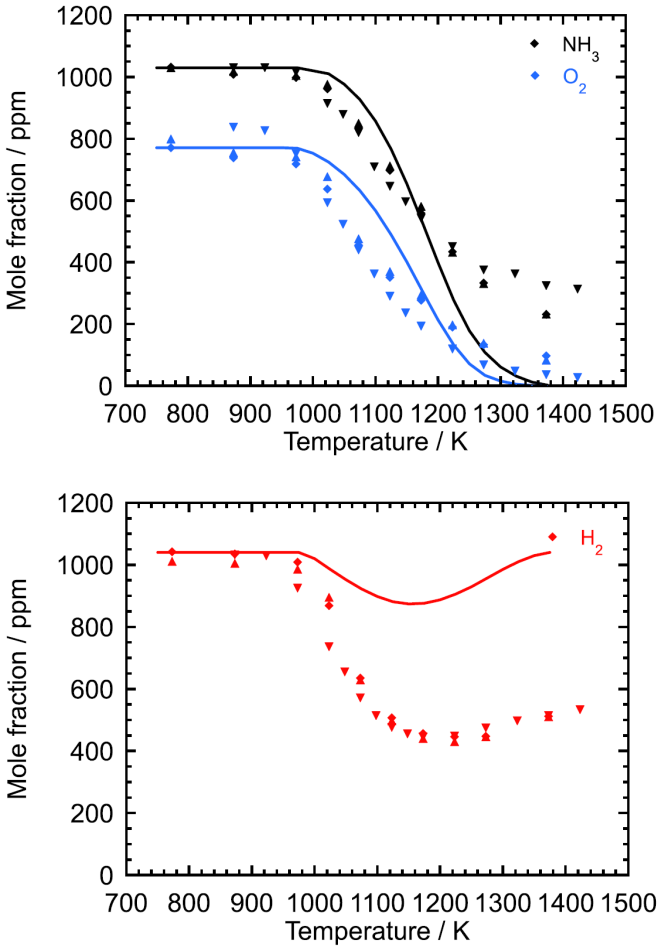

Figure 2: Comparison of experimental data from the present work with modeling predictions for oxidation of an NH_3/H_2 mixture in an atmospheric pressure non-premixed tubular flow reactor. Symbols denote experimental data (three sets under similar conditions), while solid lines denote modeling predictions. Conditions: $\diamond$ NH_3 = 1032 ppm, H_2 = 1042 ppm, O_2 = 771 ppm; $\triangle$ NH_3 = 1030 ppm, H_2 = 1011 ppm, O_2 = 799 ppm; ∇ NH_3 = 1030 ppm, H_2 = 1032 ppm, O_2 = 837 ppm; balance N_2, $\lambda \approx 0.6$; residence time (s) = 195/T(K).

predictions is shown. The model captures well the onset temperature of reaction, and the predictions of NH_3 and O_2 are mostly in satisfactory agreement with experiment. However, the consumption of H_2 above 1000 K is strongly underpredicted, while the NH_3 consumption is overpredicted above 1200 K. This discrepancy persists also for other tested mechanisms, including the recent model from Stagni et al.[50]

Figure 3 shows results for a lean mixture with approximately 1000 ppm NH_3, 500 ppm H_2, and 4000 ppm O_2. Again, reaction is initiated above 1000 K, and at 1200 K, both

NH_3 and H_2 are fully consumed. The modeling predictions agree reasonably well with the measurements, even though the H_2 oxidation rate is slightly underpredicted above 1000 K.

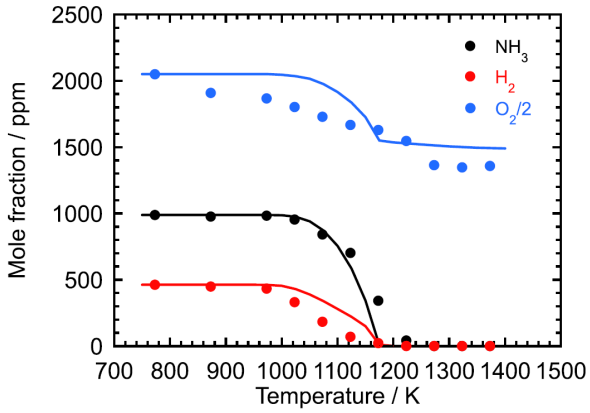

Figure 3: Comparison of experimental data from the present work with modeling predictions for oxidation of an NH_3/H_2 mixture in an atmospheric pressure non-premixed tubular flow reactor. Symbols denote experimental data, while solid lines denote modeling predictions. Conditions: $NH_3 = 988$ ppm, $H_2 = 462$ ppm, $O_2 = 4099$ ppm, balance N_2 ($\lambda = 3.2$); residence time (s) = 195/T(K).

Figure 4 shows the impact of the H_2 inlet concentration on oxidation of 1000 ppm NH_3 with 700-800 ppm O_2. Independent of the H_2 level, the onset of reaction occurs at approximately 1100 K. However, even small amounts of hydrogen significantly promotes the ammonia oxidation rate. At 1350 K, addition of 100 ppm H_2 increases the NH_3 consumption from about 10% to 40-50%, while 1000 ppm H_2 results in about 80% conversion. The kinetic model captures the observed trends, but overpredicts the oxidation at high temperature for the NH_3/H_2 mixtures.

Figure 5 shows the effect of the H_2 inlet concentration on the oxidation of 1000 ppm NH_3 under lean conditions (around 4000 ppm O_2). Contrary to the observations in Fig. 4 at lower concentrations of O_2, the H_2 level here has a strong impact on the onset temperature, which is shifted from 1300 K to 1000 K as H_2 is increased from 0 to 1850 ppm. Modeling predictions capture well the experimental observations.

Figure 6 shows the effect of the O_2 inlet concentration on the oxidation of a mixture of 1000 ppm NH_3 and 1000 ppm H_2. For all O_2 levels, oxidation is initiated at around 1050

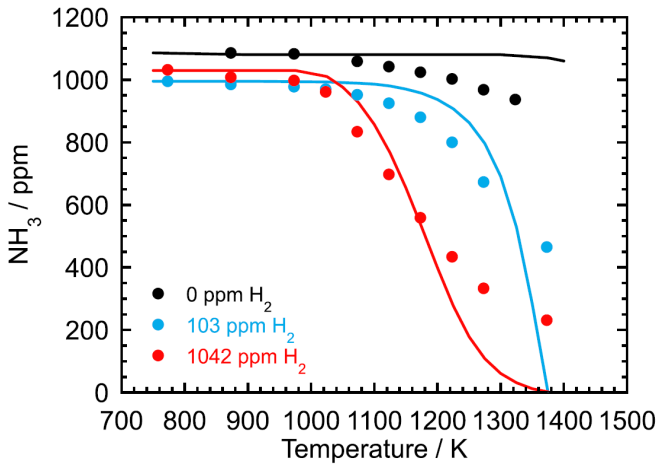

Figure 4: Comparison of experimental data from the present work with modeling predictions for oxidation of an NH_3/H_2 mixture in an atmospheric pressure non-premixed tubular flow reactor: the effect of varying the H_2 inlet concentration. Symbols denote experimental data, while solid lines denote modeling predictions. Conditions: H_2 = 0 ppm (NH_3 = 1086 ppm, O_2 = 717 ppm); H_2 = 103 ppm (NH_3 = 995 ppm, O_2 = 791 ppm); H_2 = 1042 ppm (NH_3 = 1032 ppm, O_2 = 771 ppm); balance N_2. The residence time (s) = 195/T(K).

K, but the oxidation rate increases significantly with the oxygen availability. The modeling predictions agree well with the observed NH_3 profiles.

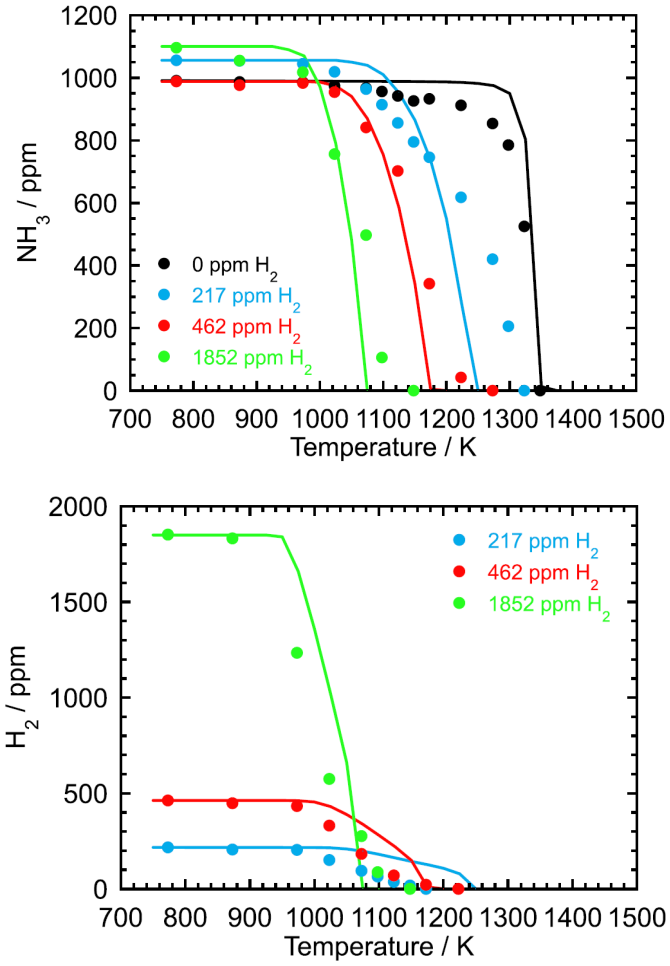

Figure 5: Comparison of experimental data from the present work with modeling predictions for oxidation of an NH_3/H_2 mixture in an atmospheric pressure non-premixed tubular flow reactor: the effect of varying the H_2 inlet concentration. Symbols denote experimental data, while solid lines denote modeling predictions. Conditions: H_2 = 0 ppm (NH_3 = 991 ppm, O_2 = 4175 ppm); H_2 = 217 ppm (NH_3 = 1056 ppm, O_2 = 3806 ppm); H_2 = 462 ppm (NH_3 = 988 ppm, O_2 = 4099 ppm); H_2 = 1852 ppm (NH_3 = 1096 ppm, O_2 = 3617 ppm); balance N_2; residence time (s) = 195/T(K).

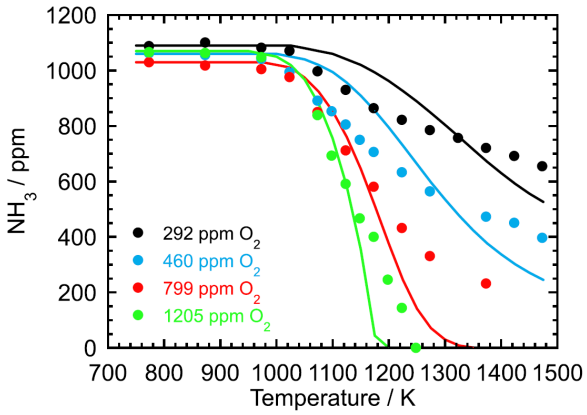

Figure 6: Comparison of experimental data from the present work with modeling predictions for oxidation of an NH_3/H_2 mixture in an atmospheric pressure non-premixed tubular flow reactor: the effect of varying the O_2 inlet concentration. Symbols denote experimental data, while solid lines denote modeling predictions. Conditions: O_2 = 292 ppm (NH_3 = 1088 ppm, H_2 = 996 ppm); O_2 = 460 ppm (NH_3 = 1062 ppm, H_2 = 977 ppm); O_2 = 799 ppm (NH_3 = 1030 ppm, H_2 = 1011 ppm); O_2 = 1205 ppm (NH_3 = 1066 ppm, H_2 = 1055 ppm); balance N_2. The residence time (s) = 195/T(K).

4.2 Premixed flow reactor results

Results from oxidation of NH_3/H_2 mixtures in premixed flow reactors have been reported by several groups. All experiments were conducted in atmospheric pressure, laminar flow tubular reactors, with a section of heating of the premixed gas, an isothermal zone, and a quenching section where the hot gas products were rapidly cooled. Most of the studies were conducted with O_2 in large excess,[46–49] but the recent studies by Zhu et al.[45] and Stagni et al.[50] involved near-stoichiometric conditions.

Similar to the non-premixed configuration discussed above, premixed experiments are generally modeled assuming isothermal plug-flow. However, hydrogen is quite reactive, particularly in the presence of a high O_2 concentration, and may be partially converted already during heating of the premixed reactants. Furthermore, break-down of the plug-flow assumption needs to be evaluated. To address these uncertainties, predictions for a plug-flow reactor, a 1D tubular reactor with laminar axial diffusion, a 1D tubular reactor with enhanced axial diffusion according to the Taylor-Aris correlation, and a 2D tubular reactor with a preheating zone were compared with the measurements of Wargadalam et al.[49] (Fig. 7). They conducted experiments with a high concentration of O_2 (10%) in a 1.2 cm diameter laminar flow reactor with a 31 cm isothermal zone. For the 1D simulations, no preheating section was included, but back-diffusion across the section (Danckwert's boundary conditions) was accounted for. In addition, calculations were conducted for a 2D axisymmetric reactor with a preheating section and with back-diffusion.

The predicted NH_3 concentration profiles are very similar among the different calculations, since at the high temperatures, where break-down of the isothermal plug-flow assumption is most pronounced, both NH_3 and H_2 are depleted before exiting the isothermal zone. The agreement between predictions and experiment for NH_3 is satisfactory, even though the model slighty overpredicts the temperature for onset of reaction.

Contrary to this, there are significant differences in the predicted NO at high temperatures. While the PFR modeling and the 1D predictions are in close agreement, the introduc-

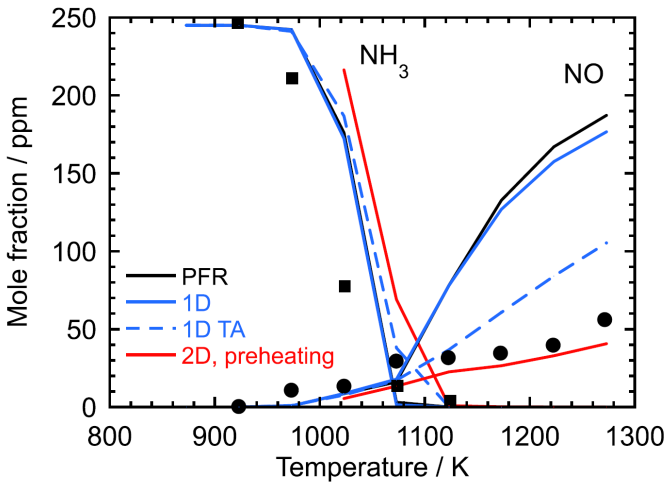

Figure 7: Comparison of experimental data from Wargadalam et al.[49] with modeling predictions for oxidation of an NH_3/H_2 mixture in a premixed atmospheric pressure tubular flow reactor under very lean conditions. Symbols denote experimental data while the solid line denotes modeling predictions, assuming isothermal plug-flow. Conditions: NH_3 = 245 ppm, H_2 = 330 ppm, O_2 = 10% (balanc N_2); isothermal zone residence time (s) = 339/T(K) (constant gas flow rate). Notation for model results: PFR (isothermal plug flow), 1D (isothermal 1D reactor with laminar axial diffusion), 1D AT (isothermal 1D reactor with enhanced axial diffusion according to the Taylor-Aris correlation), and 2D-preheating (full 2-dimensional, axisymmetric reactor, with a preheating section assumed to be 6 cm).

tion of the additional Taylor-Aris diffusion term decreases NO by about 50%. Similar to the non-premixed reactor discussed above, this is caused by a strong back-diffusion, augmented by the Taylor-Aris correction. According to the calculations, the effects of axial diffusion are not relevant along the reactor, but only at the inlet section. The 2D model, without preheating and without back-diffusion at the inlet section, yields largely the same results as the PFR model. The calculations suggest that 2D effects (radial diffusion) play a minor role at most. Similarly, the role of axial diffusion along the reactor is insignificant. However, use of the 2D model with a preheating zone results in a large reduction in the formation of NO (Fig. 7); more than a factor of four compared to the isothermal plug-flow calculation and in good agreement with experiments. Owing to its high reactivity, hydrogen is partly oxidized already during preheating, initiating consumption of NH_3 at a lower temperature and thereby limiting the formation of NO. As for the non-premixed reactor configuration, the analysis shows that experimental data for NH_3/H_2 oxidation, obtained at high temperature

in tubular flow reactors, must be interpreted with caution.

Very recently, Stagni et al.[50] investigated the impact of varying the H_2 fraction in the fuel mixture at near-stoichiometric conditions in a laminar flow reactor. Aware of the probability of reaction in the preheating region, they applied full measured temperature profiles in their modeling. Figure 8 compares the reported measurements from their study with our modeling predictions for a mixture with 1000 ppm NH_3, 1000 ppm H_2, and 1750 ppm O_2. The concentration profiles for NH_3 and H_2 are very similar under these conditions. The modeling predictions are in excellent agreement with measurements. The predictions shown in the figure are not affected by reaction during preheating.

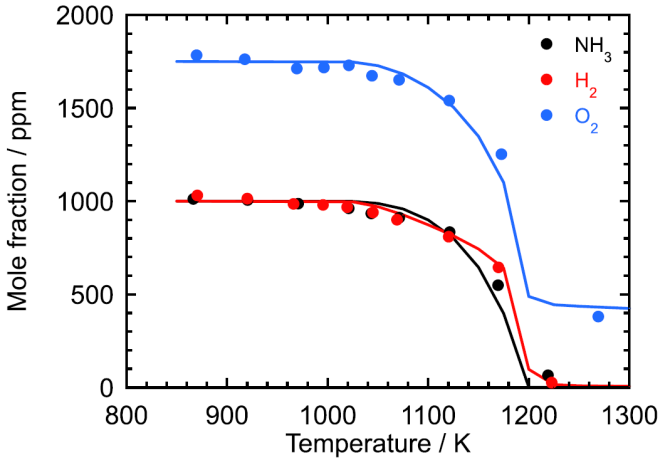

Figure 8: Comparison of experimental data from Stagni et al.[50] with modeling predictions for oxidation of an NH_3/H_2 mixture in a premixed flow reactor. Symbols denote experimental data, while solid lines denote modeling predictions. Conditions: NH_3 = 1000 ppm, H_2 = 1000 ppm, O_2 = 1750 ppm, balance N_2; pressure 1.25 atm, isothermal zone residence time = 0.05 s.

In addition to the experiments of Wargadalam et al. and Stagni et al., flow reactor studies of oxidation of NH_3/H_2 mixtures have been reported by several other groups. The results of Kasaoka et al.[46,47] were obtained in a flow reactor with the temperature varying about 100 K over the reaction zone,[83] while the studies of Zhao et al.[48] and Zhu et al.[45] involved comparatively high inlet concentrations of reactants with the risc of a considerable adiabatic temperature increase. Common for these studies is that we consider the uncertainties in the

temperature condition to be significant and we have disregarded them for model validation.

4.3 Jet-stirred reactor results

The jet-stirred reactor (JSR) is also a flow reactor, but designed to obtain intense mixing it offers reaction conditions quite different from those of the tubular reactors. Radical levels are typically higher at similar reactant levels, and ideally there is no time/spatial dependency. In the last few years, several groups have conducted experiments on NH_3/H_2 oxidation in jet-stirred reactors,[51–56] and we have included a number of these data sets in the present evaluation.

Similar to the tubular flow reactor experiments discussed above, there are uncertainties for jet-stirred reactor experiments that need to be considered as part of the kinetic interpretation. A major concern is mixing inhomogeneities, which are typically difficult to assess. Due to the high reactivity of hydrogen compared to ammonia, mixing limitations may provide a bias in the data. Another concern is reaction prior to admitting the reactants to the jet-stirred reactor itself. In most present JSR designs, reactants are diluted and the desired temperature is obtained by placing the reactor inside an electrically heated oven. Preheating the reactants before injection may facilitate reaction in the inlet system, particularly upon premixing of the reactants.

Figure 9 compares measured and predicted JSR results for oxidation of NH_3/H_2 under reducing conditions. The upper figure shows results from Osipova et al.[54] for an NH_3/H_2 ratio of 2.3 and a fuel-air equivalence ratio of $\phi = 1.5$, while data from Zhou et al.[56] for an NH_3/H_2 ratio of 1.0 and a fuel-air equivalence ratio of $\phi = 2.0$ are shown in the lower figure. In both sets of experiments, the NH_3 concentration decreases monotonically with increasing temperature, while H_2 exhibits a minimum. This behavior is qualitatively similar to that observed in Fig. 2 for the tubular reactor.

Even though the agreement between predictions and measurements is improved compared that observed for the tubular reactor (Fig. 2), similar discrepancies are observed. Above 1100

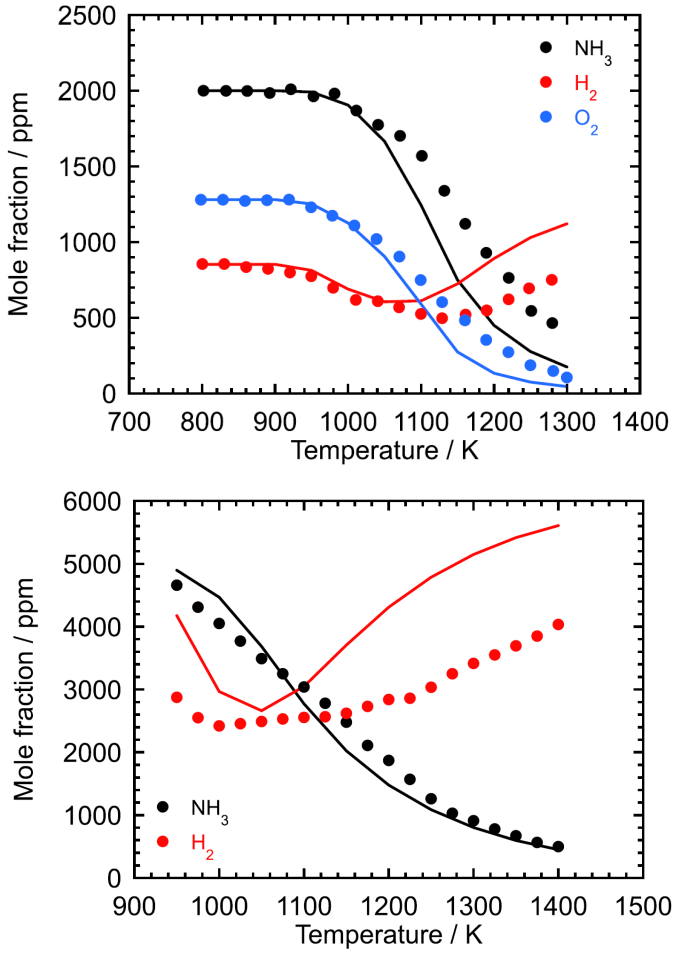

Figure 9: Comparison of experimental data with modeling predictions for oxidation of NH_3/H_2 mixtures in an atmospheric pressure jet-stirred reactor under reducing conditions. Symbols denote experimental data, while solid lines denote modeling predictions. *Upper figure:* Data from Osipova et al.[54] for 2000 ppm NH_3, 855 ppm H_2, 1925 ppm O_2 ($\phi = 1.5$); balance Ar. Residence time (s) = 1.0 s. *Lower figure:* Data from Zhou et al.[56] for 5000 ppm NH_3, 5000 ppm H_2, 3125 ppm O_2 ($\phi = 2.0$); balance N_2. Residence time (s) = 1.5 s.

K, the model overpredicts the NH_3 consumption, while the consumption of H_2 is underpredicted. The model captures better the results of Osipova et al. (Fig. 9, upper) than those of Zhou et al. (Fig. 9, lower).

Zhang et al.[52] investigated the effect of varying the H_2 fraction in the fuel mixture in the range 0-70% in a JSR. Figure 10 compares their results for NH_3/H_2 under stoichiometric conditions with modeling predictions. An increasing fraction of H_2 serves to shift the temperature range for oxidation to lower values. The modeling predictions are in good agreement

with measurements.

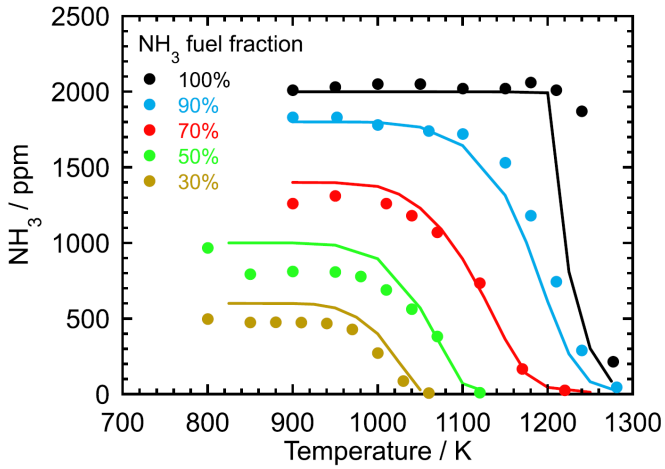

Figure 10: Comparison of experimental data with modeling predictions for oxidation of NH_3/H_2 mixtures in an atmospheric pressure jet-stirred reactor under stoichiometric conditions. Symbols denote experimental data, while solid lines denote modeling predictions. Data from Zhang et al.[52] with NH_3/H_2 varying as 100% NH_3 (2000 ppm NH_3, 0.25% O_2), 90% NH_3 (1800 ppm NH_3, 200 ppm H_2, 0.235% O_2), 80% NH_3 (1400 ppm NH_3, 600 ppm H_2, 0.205% O_2), 50% NH_3 (1000 ppm NH_3, 1000 ppm H_2, 0.175% O_2), 30% NH_3 (600 ppm NH_3, 1400 ppm H_2, 0.145% O_2); balance N_2. Residence time (s) = 1 s.

Figure 11 shows results for NH_3 obtained by Zhang et al. under lean conditions (ϕ = 0.25). Again, presence of H_2 strongly promotes reaction, with the temperature for 50% conversion decreasing from 1250 K at 100% NH_3 to about 950 K at 30% NH_3. The model captures the NH_3 profiles almost quantitatively.

He et al.[55] presented data for oxidation of NH_3/H_2 mixtures in jet-stirred reactor for a fuel-air equivalence ratio of $\phi = 0.5$ (Fig. 12). Their experiments were conducted under less dilute conditions, potentially involving a substantial heat release from reaction and thereby a larger uncertainty in the reactor temperature. The trends are similar to those shown in Fig. 11. For the experiments conducted with addition of H_2, the modeling predictions agree well with the measurements. However, the model strongly underpredicts the consumption of NH_3 in the absence of H_2, which is puzzling considering the good agreement with the data of Zhang et al. (Fig. 11). It should be noted that the shapes of the observed NH_3 profiles differ among the two sets of experiments, with the onset of reaction more steep for the Zhang et

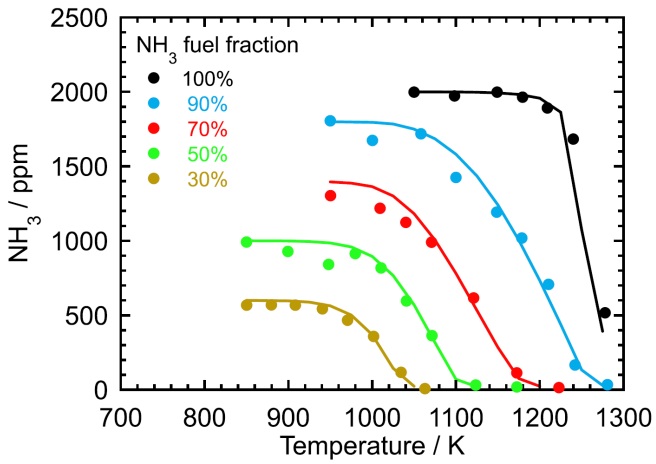

Figure 11: Comparison of experimental data from Zhang et al.[52] with modeling predictions for oxidation of NH_3/H_2 mixtures in an atmospheric pressure jet-stirred reactor under fuel-lean conditions. Symbols denote experimental data, while solid lines denote modeling predictions. Conditions: NH_3/H_2 varying as 100% NH_3 (2000 ppm NH_3, 1.0% O_2), 90% NH_3 (1800 ppm NH_3, 200 ppm H_2, 0.94% O_2), 80% NH_3 (1400 ppm NH_3, 600 ppm H_2, 0.82% O_2), 50% NH_3 (1000 ppm NH_3, 1000 ppm H_2, 0.70% O_2), 30% NH_3 (600 ppm NH_3, 1400 ppm H_2, 0.58% O_2); balance N_2. Fuel-air equivalence ratio $\phi = 0.25$; residence time (s) = 1 s.

al. data. More work is required to resolve this issue.

4.4 Premixed laminar flame structure

The flame structure of several low-pressure premixed flames fueled by ammonia/hydrogen mixtures have been reported by Vandooren and coworkers.[18–20] Figure 13 compares the measured structure of a fuel-rich premixed $NH_3/H_2/O_2/Ar$ flame from Duynslaegher et al.[20] with modeling predictions. The consumption of NH_3 and the formation of N_2 and NO are predicted well by the model. Noteworthy, also the H_2 profile is captured well, unlike the predictions from the tubular and jet-stirred flow reactors discussed above. The reason for the better agreement is perhaps related to the lower pressure in the flame or to the absence of a high-temperature mixing zone. However, the concentrations of the NH_2 radical is strongly overpredicted, while N_2O is underpredicted. Nitrous oxide is formed by the NH + NO reaction, and the discrepancy for N_2O indicates that NH is underpredicted.

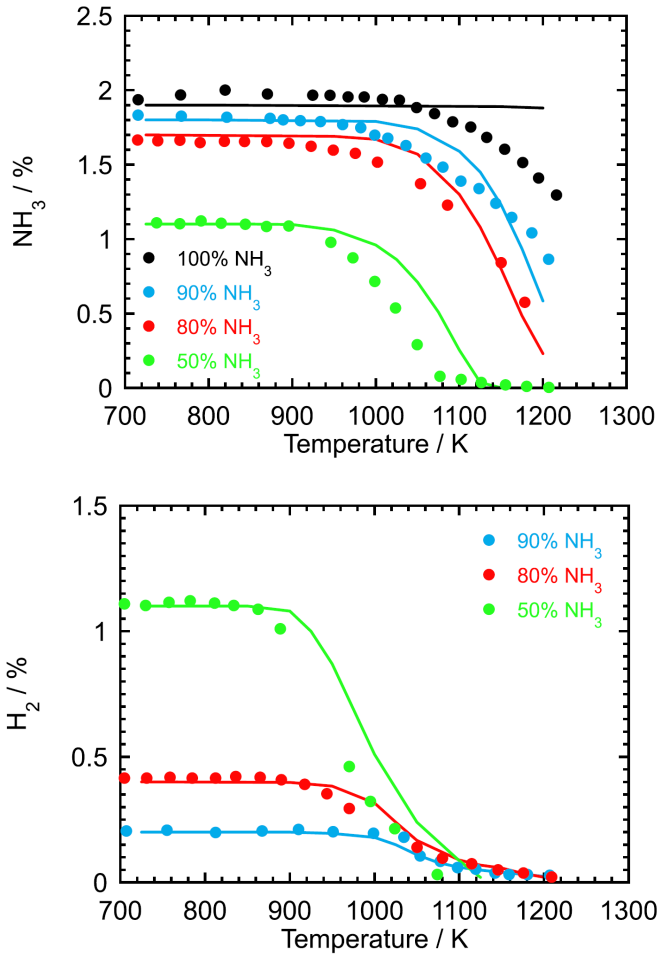

Figure 12: Comparison of experimental data from He et al.[55] with modeling predictions for oxidation of NH_3/H_2 mixtures in an atmospheric pressure jet-stirred reactor under fuel-lean conditions. Symbols denote experimental data, while solid lines denote modeling predictions. Conditions: NH_3/H_2 varying as 100% NH_3 (1.9% NH_3, 2.8% O_2), 90% NH_3 (1.8% NH_3, 0.2% H_2, 2.9% O_2), 80% NH_3 (1.7% NH_3, 0.4% H_2, 2.9% O_2), 50% NH_3: 1.1% NH_3, 1.1% H_2, 3.0% O_2; balance N_2. Fuel-air equivalence ratio $\phi = 0.5$; residence time (s) = 1 s.

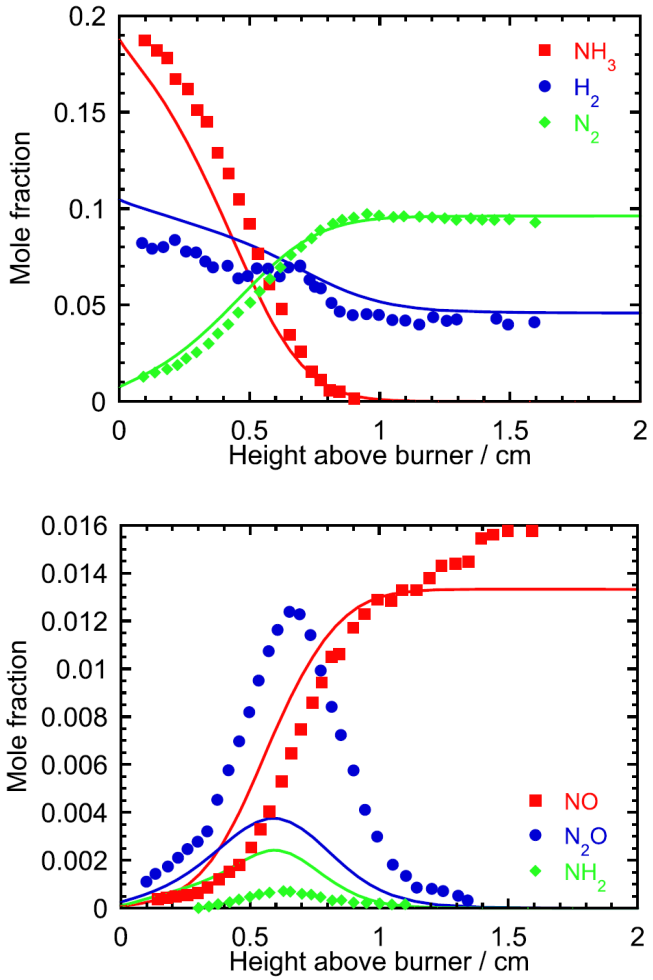

Figure 13: Comparison of the measured structure of a fuel-rich $NH_3/H_2/O_2/Ar$ flame with modeling predictions. Symbols denote experimental data from Duynslaegher et al.,[20] while solid lines denote predictions. Inlet concentrations: NH_3 = 22%, H_2 = 10%, O_2 = 20%, Ar = 48%. Pressure is 50 torr.

4.5 Analysis and further validation

The modeling predictions are generally in good agreement with the experimental data from tubular and jet-stirred reactors. However, the model underpredicts the H_2 consumption under reducing conditions, most pronounced for the tubular reactor conditions. It is presently not clear what causes this short-coming. Notably, significant deviations were reported also by Alzueta et al.[59] when modeling oxidation of CO/NH_3 mixtures under reducing conditions in a tubular reactor.

Figure 14 shows a reaction pathway diagram for NH_3 oxidation under the conditions of the present experiments. Ammonia is converted to NH_2 by reaction with the O/H radical pool, mainly OH. The NH_3 + OH reaction competes directly with H_2 + OH for the hydroxyl radical. The fate of NH_2 depends strongly on the excess air ratio, the relative levels of NH_3 and H_2, and the amount of NO formed. The NH_2 + O_2 reaction is too slow to play a role except at high O_2 concentrations. Instead, NH_2 reacts mainly with the radical pool. Under reducing conditions, NH_2 + NH_x reactions lead to formation of N_2-amines or NH, while part of the NH_2 may be recycled to NH_3 by recombination with H. Under stoichiometric and lean conditions, NH_2 is mostly oxidized to NO, through either NH or HNO. Once NO is formed in sufficient amounts, the NH_2 + NO reaction becomes the major consumption path for NH_2.

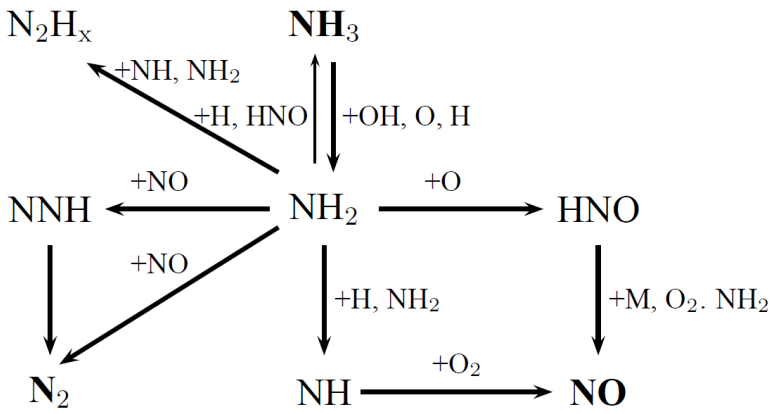

Figure 14: Reaction path diagram for oxidation of NH_3 in the presence of H_2.

The H_2 outlet concentration is controlled by the competition between consumption, pri-

marily by OH + H_2 ⇄ H_2O + H, and formation. Molecular hydrogen is formed by all H-abstraction reactions involving atomic H, primarily NH_3 + H ⇄ NH_2 + H_2 and NH_2 + H ⇄ NH + H_2. Errors in the thermodynamic properties for NH_2 and NH would affect the relative importance of the forward and reverse directions in these steps and thereby the competition between H_2 formation and consumption. However, the thermochemistry of the amine radicals is believed to be fairly well established.[65] Also addition reactions between amines and H_2 could constitute a sink for H_2. However, experimental[84,85] and theoretical[86] studies of the NH + H_2 reaction do not support stabilization of NH_3. Addition of H_2 to diazene isomers (tHNNH and H_2NN) is slow[87] and not important under our experimental conditions. Another possibility for storing hydrogen in the form of amines is formation of N_3 and N_4 amines. The pathways to formation of N_3H_5 and N_4N_6 proposed from theory by Grinberg Dana et al.[88] do not contribute significantly under the present conditions. However, addition of NH_2 to diazene isomers may play a role; more work on this issue is desirable.

Figure 15 shows the results of a sensitivity analysis for H_2 under lean and reducing conditions at 1200 K. For reducing conditions, sensitivity coefficients are shown for both tubular and jet-stirred reactors (corresponding to Figs. 2 and 9, respectively). Reaction progress is largely determined by competition between chain branching and chain terminating sequences. The competition for radicals between H_2 and NH_3 is important: H_2 + OH → H_2O + H promotes oxidation of H_2, while NH_3 + OH → NH_2 + H_2O inhibits consumption. Another important competition is between H + O_2 → O + OH (branching) and H + O_2 (+M) → HO_2 (+M) (in effect terminating). In a similar way, NH_3 + H slows down reaction by competing for atomic H with H + O_2, while NH_3 + O → NH_2 + OH is branching and promotes oxidation. Finally, even in the absence of NO in the inlet, the competition between NH_2 + NO → NNH + NO (branching) and NH_2 + NO → N_2 + H_2O (terminating) shows up as important.

The reaction path and sensitivity analyses do not provide clear indications of the reason for the poor agreement under reducing conditions between experiment and prediction. Both

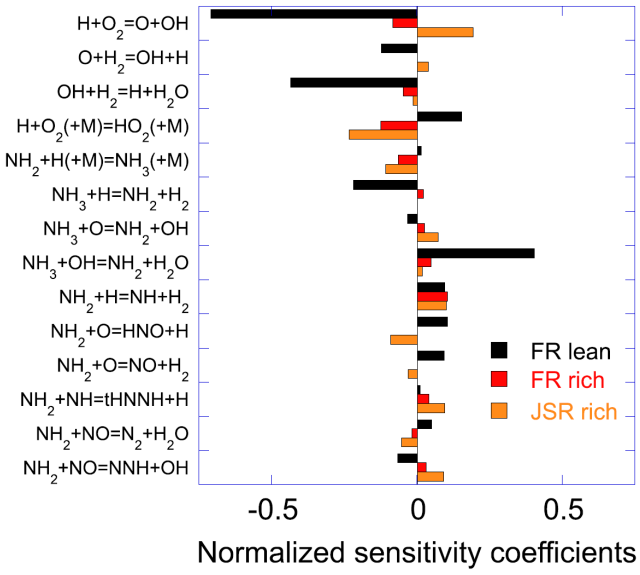

Figure 15: Sensitivity of H_2 to key reactions in oxidation of H_2/NH_3 mixtures. Conditions correspond to the lean and rich flow reactor sets in Figs. 3 and 2, respectively, and the rich JSR set in Fig. 9 (upper); all at 1200 K.

the thermochemistry of the amine radicals and the formation and reactions of N_x amines (x $\geq$ 2) should be investigated to resolve this issue. However, it should also be investigated whether a high-temperature mixing zone in the flow reactors can lead to a bias in the fuel consumption rates.

To assess the reaction mechanism at high pressure, predictions are compared to the autoignition delay times reported by Dai et al.[41] for ammonia/hydrogen mixtures in a RCM. The measurements were performed at lean and stoichiometric conditions (ϕ = 0.5 and 1.0) for compressed end gas temperatures (T_c) and pressures (P_c) of 950-1150 K and 20-60 bar, respectively. The changes in the mixture conditions that occur during the RCM experiments, such as compression and heat loss, are taken into account into the simulations. The specific volume was derived from the measured pressure trace of a nonreactive gas mixture having the same average heat capacity as the combustible mixture and used as input into the simulations, as described in detail elsewhere.[41]

The addition of hydrogen to ammonia results in a strong reduction in the ignition delay at a pressure of 60 bar, as also observed by He et al.[39] Figure 16 shows results for lean

conditions ($\phi = 0.5$). The ignition delay time measurements of the pure ammonia mixtures at lean conditions is slightly overpredicted while for the ammonia/hydrogen mixtures (5 and 10 vol% hydrogen) there is good agreement between the measurements and simulations.

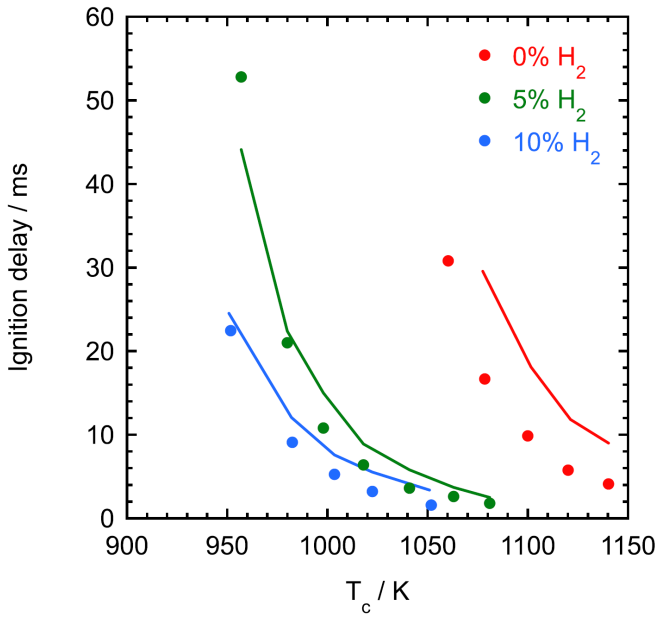

Figure 16: Comparison of measured and predicted ignition delay times as function of temperature for a fuel mixture of NH_3 with 0%, 5%, and 10% H_2 measured under lean conditions ($\phi = 0.5$) and at a compression pressure P_c of 60 bar. Experimental data from Dai et al.[41]

Figure 17 shows results for NH_3/H_2 mixtures with 10% H_2 at lean and stoichiometric conditions ($\phi = 0.5$ and 1.0) and pressures P_c of 20-60 bar. Increasing the pressure from 20 to 60 bar results in a substantial reduction in the measured and simulated autoignition delay times. The calculations capture the experimental trends but tend to overpredict the ignition delay at lower pressures. Compared to atmospheric pressure chemistry, the HO_2 radical here plays a larger role. Notably, the model presented by Dai et al. provides a better agreement with experiment than the current mechanism. The discrepancy is mostly caused by the update in the rate constants for $NH_2 + HO_2$, which is now known to be overall terminating.[64,67] The inhibition caused by $NH_2 + HO_2$ is partly compensated by the enhanced collision efficiency of NH_3 compared to N_2, in particular for H_2O_2 (+M). As discussed by Dai et al.,[41] the predicted ignition delay time is particularly sensitive to the

rate of dissociation of H_2O_2 into OH radicals.

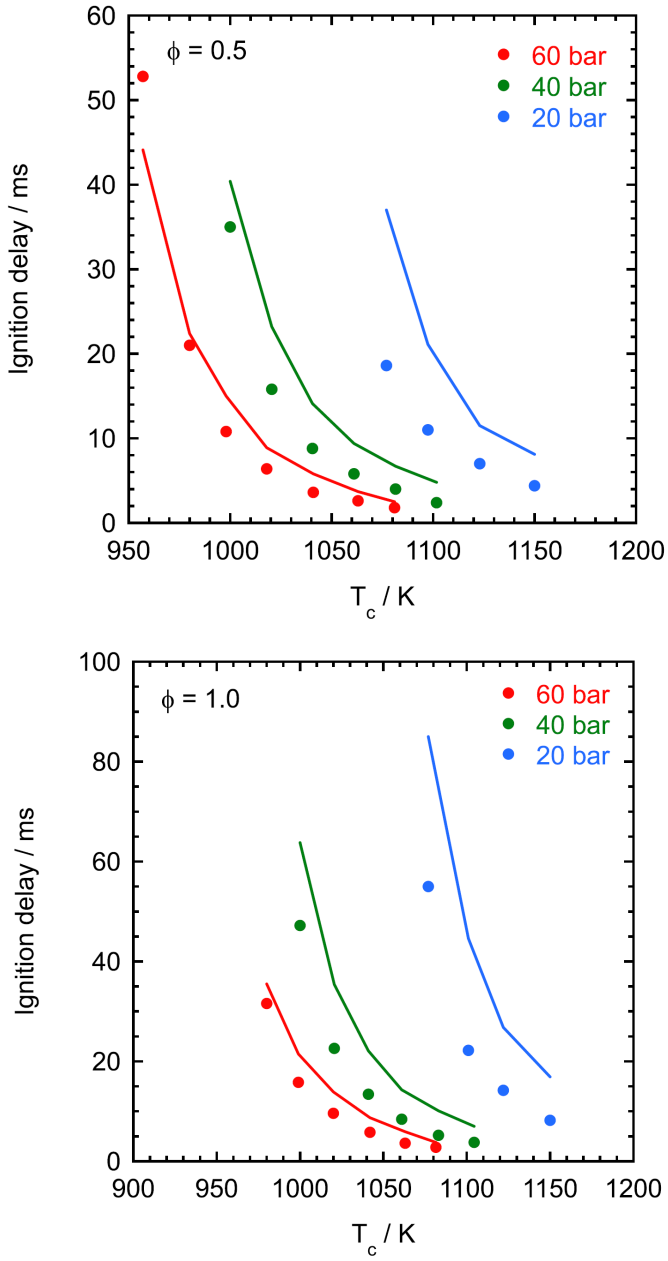

Figure 17: Comparison of measured and predicted ignition delay times as function of temperature for a fuel mixture of 90% NH_3 and 10% H_2 measured at compression pressures P_c of 20, 40 and 60 bar and equivalence ratios ϕ of 0.5 (upper) and 1.0 (lower). Experimental data from Dai et al.[41]

Figure 18 compares modeling predictions with measured flame speeds for NH_3/H_2 mixtures at atmospheric pressure. Also the speed increases strongly with the content of H_2. The

model captures quantitatively the experimental results for NH_3/H_2, while the flame speed for pure NH_3 is slightly overpredicted.

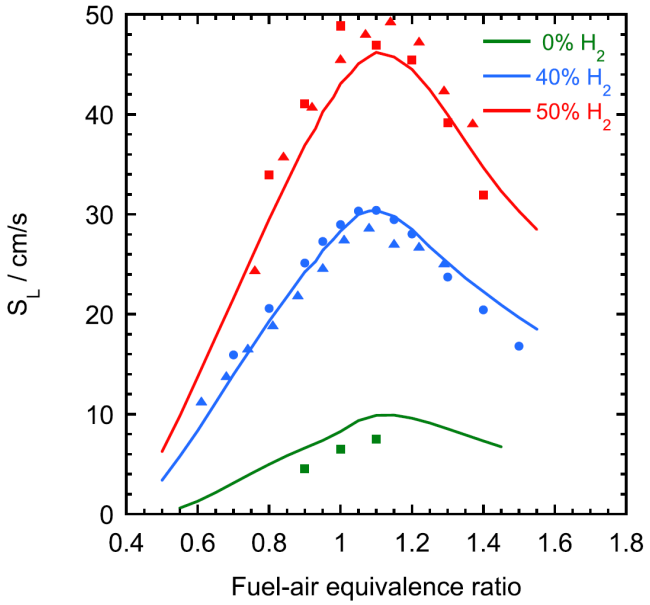

Figure 18: Comparison of measured and predicted flame speeds for NH_3/H_2 mixtures at atmospheric pressure. The experimental data are drawn from Lhuillier et al.[22] (squares), Li et al.[89] (triangles), and Wang et al.[23] (circles).

4.6 Practical implications

Use of ammonia as a fuel in maritime diesel engines is potentially the most important future application of this carbon-free energy carrier. As discussed in the Introduction, ammonia requires a co-fuel when combusted in a diesel engine due to its poor ignition and combustion properties. The most interesting co-fuels are probably diesel (available and easily ignited) and hydrogen (carbon-free, possibly made *in-situ* from catalytic NH_3 cracking). Figure 19 compares predicted ignition delay times for fuel mixtures of NH_3/H_2, NH_3/n-heptane, and $NH_3/H_2/n$-heptane under stoichiometric conditions. The n-heptane subset in the model was drawn from Zhang et al.,[90] while the subset describing amine/n-heptane interactions was adopted from Thorsen et al.[91]

The results show that both H_2 and n-heptane strongly promote ignition of NH_3. In a

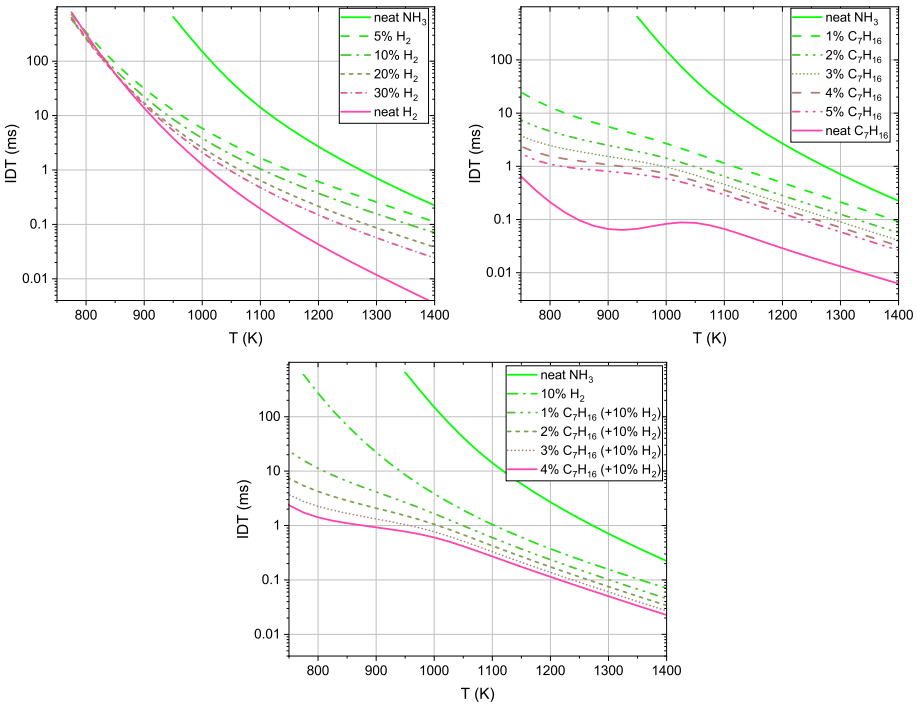

Figure 19: Predicted ignition delay times for fuel mixtures of NH_3/H_2, NH_3/n-heptane, and $NH_3/H_2/n$-heptane under stoichiometric conditions, 900 K, and 100 atm.

large 2-stroke diesel engine, the ignition conditions involve temperatures and pressures of roughly 900 K and 100 atm. As a rule of thumb, it is preferable if ignition occurs within 1 ms. According to the modeling predictions, this can be achieved under premixed conditions with an NH_3/n-heptane mixture containing 4-5% n-heptane (molar basis). However, it is notable that the ignition criterium apparently cannot be met with any fuel mixtures of NH_3/H_2: Even with pure H_2 as the fuel, the ignition delay is significantly longer than 1 ms under these conditions. For $NH_3/H_2/n$-heptane fuel mixtures, sufficiently fast ignition can be obtained with, for instance, 10% H_2 and 3-4% n-heptane. However, without diesel pilot injection, the ignition criterium is difficult to meet. The results indicate that the main benefit of adding hydrogen to the fuel mixture may be to enhance the flame speed and post-flame oxidation rate of the ammonia to shorten the combustion duration in the engine.

Conclusions

A detailed chemical kinetic model for ammonia oxidation in the presence of hydrogen has been tested against a wide range of experimental data from tubular flow reactors and jet-stirred reactors. Literature data are supplemented in the present work with novel flow reactor data on NH_3/H_2 oxidation at comparatively low reactant levels (0-2000 ppm NH_3, 0-2000 ppm H_2, 0-4000 ppm O_2), varying temperature (725-1475 K), NH_3/H_2 ratio, and excess air ratio. The agreement between prediction and experiment is good, except at reducing conditions where H_2 consumption is underpredicted. The model also provides a good prediction of NH_3/H_2 flame speeds and ignition delay times. The analysis indicates that for lean oxidation of NH_3/H_2 mixtures in premixed flow reactors, data obtained at lower temperatures can be modeled reliably assuming isothermal plug-flow. However, at higher temperatures, the selectivity for forming NO or N_2 may be affected by reaction in the inlet section prior to the isothermal zone. Modeling predictions for the high pressure, medium temperature ignition conditions in a large Diesel engine indicate that NH_3/H_2 fuel mixtures may still require a co-fuel to secure stable ignition.

Acknowledgments

M.U.A. and V.M. express their gratitude to grants PID2021-12432OB-I00 and TED2021-129557B-I00, funded by MCIN/AEI/10.13039/501100011033 and "ERDF A way of making Europe", by the "European Union" and to Aragon Government (Ref. T22_23R). S.G. kindly thanks the 'Groene Waterstof Booster' (GWB) and Zeta Energy Systems B.V for their financial support. H.H. and P.G. would like to acknowledge funding from the Danish EUDP program, the Norwegian University of Science and Technology, and Innovation Fund Denmark.

References

(1) Valera-Medina, A.; Xiao, H.; Owen-Jones, M.; David, W. I. F.; Bowen, P. J. Ammonia for power. *Prog. Energy Combust. Sci.* **2018**, *69*, 63–102.

(2) Kobayashi, H.; Hayakawa, A.; Somarathne, K. K. A.; Okafor, E. C. Science and technology of ammonia combustion. *Proc. Combust. Inst.* **2019**, *37*, 109–133.

(3) Valera-Medina, A. et al. A review on ammonia as a potential fuel: from synthesis to economics. *Energy Fuels* **2021**, *35*, 6964–7029.

(4) Chai, W. S.; Bao, Y.; Jin, P.; Tang, G.; Zhou, L. A review on ammonia, ammonia-hydrogen and ammonia-methane fuels. *Renew. Sustain. Energy Rev.* **2021**, *147*, 111254.

(5) Kang, L.; Pan, W.; Zhang, J.; Wang, W.; Tang, C. A review on ammonia blends combustion for industrial applications. *Fuel* **2023**, *332*, 126150.

(6) Awad, O. I.; Zhou, B.; Harrath, K.; Kadirgama, K. Characteristics of NH_3/H_2 blend as carbon-free fuels: A review. *Int. J. Hydrogen Energy* **2023**, in press.

(7) Greenblatt, D.; Tian, L.; Lindstedt, R. P. The impact of hydrogen substitution by ammonia on low-and high-temperature combustion. *Combust. Flame* **2023**, *257*, 112733.

(8) Manigandan, S.; Ryu, J. I.; Praveen Kumar, T. R.; Elgendi, M. Hydrogen and ammonia as a primary fuel – A critical review of production technologies, diesel engine applications, and challenges. *Fuel* **2023**, *352*, 129100.

(9) Mathieu, O.; Petersen, E. L. Experimental and modeling study on the high-temperature oxidation of ammonia and related NO_x chemistry. *Combust. Flame* **2015**, *162*, 554–570.

(10) Li, J.; Huang, H.; Kobayashi, N.; Wang, C.; Yuan, H. Numerical study on laminar burning velocity and ignition delay time of ammonia flame with hydrogen addition. *Energy* **2017**, *126*, 796–809.

(11) Otomo, J.; Koshi, M.; Mitsumori, T.; Iwasaki, H.; Yamada, K. Chemical kinetic modeling of ammonia oxidation with improved reaction mechanism for ammonia/air and ammonia/hydrogen/air combustion. *Int. J. Hydrogen Energy* **2018**, *43*, 3004–3014.

(12) Glarborg, P.; Miller, J.; Ruscic, B.; Klippenstein, S. Modeling nitrogen chemistry in combustion. *Prog. Energy Combust. Sci.* **2018**, *67*, 31–68.

(13) Mei, B.; Zhang, X.; Ma, S.; Cui, M.; Guo, H.; Cao, Z.; Li, Y. Experimental and kinetic modeling investigation on the laminar flame propagation of ammonia under oxygen enrichment and elevated pressure conditions. *Combust. Flame* **2019**, *210*, 236–246.

(14) Mei, B.; Zhang, J.; Shi, X.; Xi, Z.; Li, Y. Enhancement of ammonia combustion with partial fuel cracking strategy: Laminar flame propagation and kinetic modeling investigation of $NH_3/H_2/N_2$/air mixtures up to 10 atm. *Combust. Flame* **2021**, *231*, 111472.

(15) Stagni, A.; Cavallotti, C.; Arunthanayothin, S.; Song, Y.; Herbinet, O.; Battin-Leclerc, F.; Faravelli, T. An experimental, theoretical and kinetic-modeling study of the gas-phase oxidation of ammonia. *Reaction Chem. Eng.* **2020**, *5*, 696–711.

(16) Jiang, Y.; Gruber, A.; Seshadri, K.; Williams, F. An updated short chemical-kinetic nitrogen mechanism for carbon-free combustion applications. *Int. J. Energy Res.* **2020**, *44*, 795–810.

(17) Aganesyan, K. T.; Nalbandyan, A. B. Determination of the rate constants in the reactions of H and O atoms with the NH_3 molecule. *Dokl. Akad. Nauk* **1965**, *160*, 162–165.

(18) Bian, J.; Vandooren, J.; Van Tiggelen, P. J. Experimental study of the formation of nitrous and nitric oxides in H_2 - O_2 - Ar flames seeded with NO and/or NH_3. *Symp. (Int.) Combust.* **1991**, *23*, 379–386.

(19) Vandooren, J. Comparison of the experimental structure of an ammonia seeded rich

hydrogen-oxygen-argon flame with the calculated ones along several reaction mechanisms. *Combust. Sci. Technol.* **1992**, *84*, 335–344.

(20) Duynslaegher, C.; Jeanmart, H.; Vandooren, J. Flame structure studies of premixed ammonia/hydrogen/oxygen/argon flames: Experimental and numerical investigation. *Proc. Combust. Inst.* **2009**, *32*, 1277–1284.

(21) Kumar, P.; Meyer, T. R. Experimental and modeling study of chemical-kinetics mechanisms for H_2–NH_3–air mixtures in laminar premixed jet flames. *Fuel* **2013**, *108*, 166–176.

(22) Lhuillier, C.; Brequigny, P.; Lamoureux, N.; Contino, F.; Mounaïm-Rousselle, C. Experimental investigation on laminar burning velocities of ammonia/hydrogen/air mixtures at elevated temperatures. *Fuel* **2020**, *263*, 116653.

(23) Wang, S.; Wang, Z.; Elbaz, A. M.; Han, X.; He, Y.; Costa, M.; Konnov, A. A.; Roberts, W. L. Experimental study and kinetic analysis of the laminar burning velocity of NH_3/syngas/air, NH_3/CO/air and NH_3/H_2/air premixed flames at elevated pressures. *Combust. Flame* **2020**, *221*, 270–287.

(24) Shrestha, K. P.; Lhuillier, C.; Barbosa, A. A.; Brequigny, P.; Contino, F.; Mounaïm-Rousselle, C.; Seidel, L.; Mauss, F. An experimental and modeling study of ammonia with enriched oxygen content and ammonia/hydrogen laminar flame speed at elevated pressure and temperature. *Proc. Combust. Inst.* **2021**, *38*, 2163–2174.

(25) Wang, N.; Huang, S.; Zhang, Z.; Li, T.; Yi, P.; Wu, D.; Chen, G. Laminar burning characteristics of ammonia/hydrogen/air mixtures with laser ignition. *Int. J. Hydrogen Energy* **2021**, *46*, 31879–31893.

(26) Gotama, G. J.; Hayakawa, A.; Okafor, E. C.; Kanoshima, R.; Hayashi, M.; Kudo, T.; Kobayashi, H. Measurement of the laminar burning velocity and kinetics study of the

importance of the hydrogen recovery mechanism of ammonia/hydrogen/air premixed flames. *Combust. Flame* **2022**, *236*, 111753.

(27) Osipova, K. N.; Korobeinichev, O. P.; Shmakov, A. G. Chemical structure and laminar burning velocity of atmospheric pressure premixed ammonia/hydrogen flames. *Int. J. Hydrogen Energy* **2021**, *46*, 39942–39954.

(28) Jin, B.-z.; Deng, Y.-F.; Li, G.-x.; Li, H.-m. Experimental and numerical study of the laminar burning velocity of NH_3/H_2/air premixed flames at elevated pressure and temperature. *Int. J. Hydrogen Energy* **2022**, *47*, 36046–36057.

(29) Ji, C.; Wang, Z.; Wang, D.; Hou, R.; Zhang, T.; Wang, S. Experimental and numerical study on premixed partially dissociated ammonia mixtures. Part I: Laminar burning velocity of $NH_3/H_2/N_2$/air mixtures. *Int. J. Hydrogen Energy* **2022**, *47*, 4171–4184.

(30) Li, H.; Xiao, H.; Sun, J. Laminar burning velocity, Markstein length, and cellular instability of spherically propagating NH_3/H_2/Air premixed flames at moderate pressures. *Combust. Flame* **2022**, *241*, 112079.

(31) Han, X.; Wang, Z.; He, Y.; Zhu, Y.; Lin, R.; Konnov, A. A. Uniqueness and similarity in flame propagation of pre-dissociated NH_3 + air and NH_3 + H_2 + air mixtures: An experimental and modelling study. *Fuel* **2022**, *327*, 125159.

(32) Wu, Z.; Lv, J.; Liu, X.; Wu, W.; Zhou, S.; Yan, B.; Chen, G. Adiabatic laminar burning velocities and NO generation paths of NH_3/H_2 premixed flames. *J. Energy Inst.* **2023**, *108*, 101225.

(33) Chen, X.; Liu, Q.; Zhao, W.; Li, R.; Zhang, Q.; Mou, Z. Experimental and chemical kinetic study on the flame propagation characteristics of ammonia/hydrogen/air mixtures. *Fuel* **2023**, *334*, 126509.

(34) Wang, Z.; Ji, C.; Zhang, T.; Wang, D.; Zhai, Y.; Wang, S. Experimental and numerical study on laminar premixed $NH_3/H_2/O_2$/air flames. *Int. J. Hydrogen Energy* **2023**, *48*, 14885–14895.

(35) Zhou, S.; Cui, B.; Yang, W.; Tan, H.; Wang, J.; Dai, H.; Li, L.; Rahman, Z. U.; Wang, X.; Deng, S.; Wang, X. An experimental and kinetic modeling study on NH_3/air, NH_3/H_2/air, NH_3/CO/air, and NH_3/CH_4/air premixed laminar flames at elevated temperature. *Combust. Flame* **2023**, *248*.

(36) Joo, J. M.; Lee, S.; Kwon, O. C. Effects of ammonia substitution on combustion stability limits and NO_x emissions of premixed hydrogen-air flames. *Int. J. Hydrogen Energy* **2012**, *37*, 6933–6941.

(37) Alfazazi, A.; Es-sebbar, E.-t.; Zhang, X.; Dally, B.; Abdullah, M.; Younes, M.; Sarathy, S. M. Counterflow flame extinction of ammonia and its blends with hydrogen and C1-C3 hydrocarbons. *Appl. Energy Combust. Sci.* **2022**, *12*, 100099.

(38) Richter, M.; Schultheis, R.; Dawson, J. R.; Gruber, A.; Barlow, R. S.; Dreizler, A.; Geyer, D. Extinction strain rates of premixed ammonia/hydrogen/nitrogen-air counterflow flames. *Proc. Combust. Inst.* **2023**, *39*, 2027–2035.

(39) He, X.; Shu, B.; Nascimento, D.; Moshammer, K.; Costa, M.; Fernandes, R. X. Autoignition kinetics of ammonia and ammonia/hydrogen mixtures at intermediate temperatures and high pressures. *Combust. Flame* **2019**, *206*, 189–200.

(40) Pochet, M.; Dias, V.; Moreau, B.; Foucher, F.; Jeanmart, H.; Contino, F. Experimental and numerical study, under LTC conditions, of ammonia ignition delay with and without hydrogen addition. *Proc. Combust. Inst.* **2019**, *37*, 621–629.

(41) Dai, L.; Gersen, S.; Glarborg, P.; Levinsky, H.; Mokhov, A. Experimental and numerical analysis of the autoignition behavior of NH_3 and NH_3/H_2 mixtures at high pressure. *Combust. Flame* **2020**, *215*, 134–144.

(42) Liao, W.; Chu, Z.; Wang, Y.; Li, S.; Yang, B. An experimental and modeling study on auto-ignition of ammonia in an RCM with N_2O and H_2 addition. *Proc. Combust. Inst.* **2023**, *39*, 4377–4385.

(43) Chen, J.; Jiang, X.; Qin, X.; Huang, Z. Effect of hydrogen blending on the high temperature auto-ignition of ammonia at elevated pressure. *Fuel* **2021**, *287*, 119563.

(44) Alturaifi, S. A.; Mathieu, O.; Petersen, E. L. A shock-tube study of NH_3 and NH_3/H_2 oxidation using laser absorption of NH_3 and H_2O. *Proc. Combust. Inst.* **2023**, *39*, 233–241.

(45) Zhu, D.; Ruwe, L.; Schmitt, S.; Shu, B.; Kohse-Hoinghaus, K.; Lucassen, A. Interactions in ammonia and hydrogen oxidation examined in a flow reactor and a shock tube. *J. Phys. Chem. A* **2023**, *127*, 2351–2366.

(46) Kasaoka, S.; Sasaoka, E.; Nagahiro, M. Non-catalytic reduction of nitrogen monoxide with ammonia and oxidation of ammonia with oxygen under coexistence of hydrogen. *Nippon Kagaku Kaishi* **1979**, *5*, 668–674.

(47) Kasaoka, S.; Sasaoka, E.; Ikoma, M. Effect of addition of carbon monoxide and hydrogen on non-catalytic reduction of nitrogen monoxide with ammonia. *Nippon Kagaku Kaishi* **1981**, *4*, 597–604.

(48) Zhao, Z. S.; Matsuda, H.; Arai, N.; Hasatani, M. Mechanism of NH_3 Oxidation in $NH_3/H_2/O_2/Ar$ Gas System. *Kagaku Kogaku Ronbunshu* **1991**, *17*, 828–836.

(49) Wargadalam, V. J.; Löffler, G.; Winter, F.; Hofbauer, H. Homogeneous formation of NO and N_2O from the oxidation of HCN and NH_3 at 600-1000^{o}C. *Combust. Flame* **2000**, *120*, 465–478.

(50) Stagni, A.; Arunthanayothin, S.; Dehue, M.; Herbinet, O.; Battin-Leclerc, F.; Bréquigny, P.; Mounaïm-Rousselle, C.; Faravelli, T. Low-and intermediate-temperature

ammonia/hydrogen oxidation in a flow reactor: Experiments and a wide-range kinetic modeling. *Chem. Eng. J.* **2023**, *471*, 144577.

(51) Ding, C.; Li, P.; Wang, K.; Shi, G.; Wang, F.; Liu, Z. Experimental and Kinetic Study on the Oxidation of Syngas-Ammonia under both N_2 and CO_2 Atmospheres in a Jet-Stirred Reactor. *Energy Fuels* **2021**, *35*, 11445–11456.

(52) Zhang, X.; Moosakutty, S. P.; Rajan, R. P.; Younes, M.; Sarathy, S. M. Combustion chemistry of ammonia/hydrogen mixtures: Jet-stirred reactor measurements and comprehensive kinetic modeling. *Combust. Flame* **2021**, *234*, 111653.

(53) Manna, M. V.; Sabia, P.; Sorrentino, G.; Viola, T.; Ragucci, R.; de Joannon, M. New insight into NH_3-H_2 mutual inhibiting effects and dynamic regimes at low-intermediate temperatures. *Combust. Flame* **2022**, *243*, 111957.

(54) Osipova, K. N.; Zhang, X.; Sarathy, S. M.; Korobeinichev, O. P.; Shmakov, A. G. Ammonia and ammonia/hydrogen blends oxidation in a jet-stirred reactor: Experimental and numerical study. *Fuel* **2022**, *310*, 122202.

(55) He, X.; Li, M.; Shu, B.; Fernandes, R.; Moshammer, K. Exploring the effect of different reactivity promoters on the oxidation of ammonia in a jet-stirred reactor. *J. Phys. Chem. A* **2023**, *127*, 1923–1940.

(56) Zhou, S.; Yang, W.; Zheng, S.; Yu, S.; Tan, H.; Cui, B.; Wang, J.; Deng, S.; Wang, X. An experimental and kinetic modeling study on the low and intermediate temperatures oxidation of $NH_3/O_2/Ar$, $NH_3/H_2/O_2/Ar$, $NH_3/CO/O_2/Ar$, and $NH_3/CH_4/O_2/Ar$ mixtures in a jet-stirred reactor. *Combust. Flame* **2023**, *248*, 112529.

(57) Jian, J.; Hashemi, H.; Wu, H.; Glarborg, P.; Jasper, A. W.; Klippenstein, S. J. An experimental, theoretical, and kinetic modeling study of post-flame oxidation of ammonia. *submitted for publication* **2023**,

(58) Glarborg, P. The $NH_3/NO_2/O_2$ system: Constraining key steps in ammonia ignition and N_2O formation. *Combust. Flame* **2023**, *257*, 112311.

(59) Alzueta, M. U.; Salas, I.; Hashemi, H.; Glarborg, P. CO assisted NH_3 oxidation. *Combust. Flame* **2023**, *257*, 112438.

(60) Burke, M. P.; Chaos, M.; Ju, Y.; Dryer, F. L.; Klippenstein, S. J. Comprehensive H_2/O_2 kinetic model for high-pressure combustion. *Int. J. Chem. Kinet.* **2012**, *44*, 444–474.

(61) Hashemi, H.; Christensen, J. M.; Gersen, S.; Glarborg, P. Hydrogen oxidation at high pressure and intermediate temperatures: Experiments and kinetic modeling. *Proc. Combust. Inst.* **2015**, *35*, 553–560.

(62) Burke, M. P.; Klippenstein, S. J. Ephemeral collision complexes mediate chemically termolecular transformations that affect system chemistry. *Nat. Chem.* **2017**, *9*, 1078–1082.

(63) Klippenstein, S. J.; Sivaramakrishnan, R.; Burke, U.; Somers, K. P.; Curran, H. J.; Cai, L.; Pitsch, H.; Pelucchi, M.; Faravelli, T.; Glarborg, P. $HO_2 + HO_2$: High level theory and the role of singlet channels. *Combust. Flame* **2022**, *243*, 111975.

(64) Glarborg, P.; Hashemi, H.; Cheskis, S.; Jasper, A. W. On the rate constant for $NH_2 + HO_2$ and third-body collision efficiencies for $NH_2 + H$ (+ M) and $NH_2 + NH_2$ (+ M). *J. Phys. Chem. A* **2021**, *125*, 1505–1516.

(65) Glarborg, P.; Hashemi, H.; Marshall, P. Challenges in kinetic modeling of ammonia pyrolysis. *Fuel Commun.* **2022**, *10*, 100049.

(66) Klippenstein, S. J.; Mulvihill, C. R.; Glarborg, P. Theoretical kinetics predictions for reactions on the NH_2O potential energy surface. *J. Phys. Chem. A* **2023**, *127*, 8650–8662.

(67) Klippenstein, S. J.; Glarborg, P. Theoretical kinetics predictions for NH_2 + HO_2. *Combust. Flame* **2022**, *236*, 111787.

(68) Marshall, P.; Rawling, G.; Glarborg, P. New reactions of diazene and related species for modelling combustion of amine fuels. *Mol. Phys.* **2021**, *119*, e1979674.

(69) Stagni, A.; Cavallotti, C. H-abstractions by O_2, NO_2, NH_2, and HO_2 from H_2NO: Theoretical study and implications for ammonia low-temperature kinetics. *Proc. Combust. Inst.* **2023**, *39*, 633–641.

(70) Jasper, A. W. Predicting third-body collision efficiencies for water and other polyatomic baths. *Faraday Discuss.* **2022**, *238*, 68–86.

(71) Alzueta, M. U.; Hernández, J. M. Ethanol oxidation and its interaction with nitric oxide. *Energy Fuels* **2002**, *16*, 166–171.

(72) Alzueta, M. U.; Pernia, R.; Abian, M.; Millera, A.; Bilbao, R. CH_3SH conversion in a tubular flow reactor. Experiments and kinetic modelling. *Combust. Flame* **2019**, *203*, 23–30.

(73) Abián, M.; Benés, M.; de Goñi, A.; Muñoz, B.; Alzueta, M. U. Study of the oxidation of ammonia in a flow reactor. Experiments and kinetic modeling simulation. *Fuel* **2021**, *300*, 120979.

(74) Alzueta, M. U.; Glarborg, P.; Dam-Johansen, K. Low temperature interactions between hydrocarbons and nitric oxide: An experimental study. *Combust. Flame* **1997**, *109*, 25–36.

(75) Dean, A. M.; Hardy, J. E.; Lyon, R. K. Kinetics and mechanism of NH_3 oxidation. *Symp. (Int.) Combust.* **1982**, *19*, 97–105.

(76) Ansys Chemkin-PRO 2022 R2. 2022.

(77) Cuoci, A.; Frassoldati, A.; Faravelli, T.; Ranzi, E. OpenSMOKE++: An object-oriented framework for the numerical modeling of reactive systems with detailed kinetic mechanisms. *Computer Phys. Commun.* **2015**, *192*, 237–264.

(78) Cuoci, A. *Computer Aided Chemical Engineering*; Elsevier, 2019; Vol. 45; pp 675–721.

(79) Cuoci, A.; Frassoldati, A.; Faravelli, T.; Ranzi, E. Numerical modeling of laminar flames with detailed kinetics based on the operator-splitting method. *Energy Fuels* **2013**, *27*, 7730–7753.

(80) Cuoci, A.; Frassoldati, A.; Faravelli, T.; Ranzi, E. A computational tool for the detailed kinetic modeling of laminar flames: Application to C_2H_4/CH_4 coflow flames. *Combust. Flame* **2013**, *160*, 870–886.

(81) Kristensen, P. G.; Glarborg, P.; Dam-Johansen, K. Nitrogen chemistry during burnout in fuel-staged combustion. *Combust. Flame* **1996**, *107*, 211–222.

(82) Levenspiel, O. *Chemical Reaction Engineering (3rd Edition)*; Wiley, 1998; p 311.

(83) Kasaoka, S.; Sasaoka, E.; Nagahiro, M.; Kawakami, K. Non-catalytic reduction of nitrogen monoxide with ammonia and oxidation of ammonia with oxygen. *Nippon Kagaku Kaishi* **1979**, 138–144.

(84) Röhrig, M.; Wagner, H. G. The reactions of NH ($X^3\Sigma$-) with the water gas components CO_2, H_2O, and H_2. *Symp. (Int.) Combust.* **1994**, *25*, 975–981.

(85) Fontijn, A.; Shamsuddin, S. M.; Crammond, D.; Marshall, P.; Anderson, W. R. Kinetics of the NH reaction with H_2 and reassessment of HNO formation from NH + CO_2, H_2O. *Combust. Flame* **2006**, *145*, 543–551.

(86) Mackie, J. C.; Bacskay, G. B. Quantum chemical study of the mechanism of reaction between NH ($X^3\Sigma$-) and H_2, H_2O, and CO_2 under combustion conditions. *J. Phys. Chem. A* **2005**, *109*, 11967–11974.

(87) Hwang, D.-Y.; Mebel, A. M. Reaction mechanism of N_2/H_2 conversion to NH_3: a theoretical study. *J. Phys. Chem. A* **2003**, *107*, 2865–2874.

(88) Grinberg Dana, A.; Moore III, K. B.; Jasper, A. W.; Green, W. H. Large intermediates in hydrazine decomposition: A theoretical study of the N_3H_5 and N_4H_6 potential energy surfaces. *J. Phys. Chem. A* **2019**, *123*, 4679–4692.

(89) Li, J.; Huang, H.; Kobayashi, N.; He, Z.; Nagai, Y. Study on using hydrogen and ammonia as fuels: Combustion characteristics and NO_x formation. *Int. J. Energy Res.* **2014**, *38*, 1214–1223.

(90) Zhang, K.; Banyon, C.; Bugler, J.; Curran, H. J.; Rodriguez, A.; Herbinet, O.; Battin-Leclerc, F.; B'Chir, C.; Heufer, K. A. An updated experimental and kinetic modeling study of n-heptane oxidation. *Combust, Flame* **2016**, *172*, 116–135.

(91) Thorsen, L. S.; Jensen, M. S. T.; Pullich, M. S.; Christensen, J. M.; Hashemi, H.; Glarborg, P.; Alekseev, V. A.; Nilsson, E. J. K.; Wang, Z.; Mei, B.; Liu, N.; Ju, Y. High pressure oxidation of NH_3/*n*-heptane mixtures. *Combust. Flame* **2023**, *254*, 112785.